Wideband Indoor Channel Measurements and BER Analysis of Frequency Selective Multipath Channels at 2.4, 4.75, and 11.5 GHz

Gerard J. M. Janssen, *Member, IEEE,* Patrick A. Stigter, and Ramjee Prasad, *Senior Member, IEEE*

***Abstract*—Results from propagation measurements, conducted in an indoor office environment at 2.4, 4.75, and 11.5 GHz, are presented. The data were obtained in small clusters of six measurements, using a coherent wideband measurement system. The channel characteristics for the three frequencies are compared by evaluating path loss, rms delay spread, and coherence bandwidth.**

An analytical model for evaluation of the bit-error rate (BER) of the stationary frequency selective indoor channel is developed for a coherent binary phase shift keying (BPSK) receiver, based on the complex impulse response of the channel. Computational BER results are obtained for data rates up to 50 Mb/s, using the measured multipath channel impulse responses. The BER results for a number of clusters are presented and compared for the maximum reliable datarate as inferred by the measured rms delay spread of the channel.

I. Introduction

THE interest in indoor wireless communications (IWC) has grown rapidly in recent years because of the advantages over cable networks, such as mobility of users, elimination of cabling, flexibility of changing, and creating various new communication services. IWC offers highly attractive means of combined voice and data transmissions in business environments. Therefore, intensive studies of the IWC environment have drawn the attentions of many researchers for both propagation measurements and theoretical analysis [1]–[14].

In indoor radio communication, special propagation problems arise due to the highly reflective and shadowing environment, which are related to the problems also present in outdoor mobile communication. In the indoor channel, which depends heavily on the type of building (materials, dimensions, etc.), radio signals propagate via multiple paths which differ in amplitude, phase, and delay time. Therefore, the received information signal is distorted by time dispersion and amplitude fading. These anomalies limit the maximum channel symbol rate significantly when no special precautions are taken, e.g., adaptive equalization or antenna diversity. Recently, radio propagation measurements in the indoor radio channel were reported by several researchers [1]–[8]. These propagation measurements were conducted in different types of buildings at frequencies 900 MHz, 1.7 GHz, 4.0 GHz, and 5.8 GHz.

In the first part of this paper, the results of coherent wideband propagation measurements, which have been conducted simultaneously at 2.4, 4.75, and 11.5 GHz in wideband indoor channels, are presented. The effect of frequency on path loss, root mean square (rms) delay spread and coherence bandwidth is evaluated. In this paper we will use the terms wideband and narrowband to indicate that the occupied bandwidth for measurements or information transmission is larger or smaller, respectively, than the coherence bandwidth of the channel.

In the second part of the paper, a theoretical model for evaluation of the bit-error rate (BER) of the stationary frequency selective indoor channel is developed for the coherent binary phase shift keying (BPSK) receiver. This model is used to compute BER results for data rates up to 50 Mb/s, using measured complex channel impulse responses, at 2.4, 4.75, and 11.5 GHz.

The content of this paper is organized as follows. In Section II, the indoor multipath channel model is briefly reviewed, and important channel parameters are discussed. Propagation measurement results for the indoor wideband channel at 2.4, 4.75, and 11.5 GHz of an indoor laboratory/office environment,[1] are presented in Section III. The measurement principle, the measurement system and the indoor environment are described in detail. The measurement results and values for the path loss law, rms delay spread (τ_{rms}) and coherence bandwidth (B_{coh}) are given for three different situation viz.: line-of-sight (LOS), obstructed direct path (OBS), and the effect of people being present in the room. A summary of these results was presented in [9]. In Section IV, an analytical BER model for the stationary frequency selective multipath channel is derived for the coherent BPSK receiver. In this model the measured channel impulse response is used. Numerical BER results for a number of measured indoor channels are given. Finally, conclusions are given in Section V.

II. The Indoor Radio Channel

The indoor radio channel is an adverse communication channel, which causes undesired frequency selective fading and dispersion of the information signal. The baseband com-

Paper approved by J. Weitzen, the Editor for Fading/Equalization of the IEEE Communications Society. Manuscript received November 15, 1993; revised November 15, 1994. This paper was presented in part at the 42nd IEEE Vehicular Technology Society Conference, Denver, CO, May 1992, and the 3rd IEEE Communications Theory Mini-Conference of GLOBECOM'94, San Francisco, CA, November 1994.

The authors are with the Telecommunications and Traffic Control Systems Group, Delft University of Technology, The Netherlands.

Publisher Item Identifier S 0090-6778(96)07372-2.

[1] The measurements have been conducted at the TNO Physics and Electronics Laboratory, The Hague, The Netherlands.

plex channel impulse response is modeled as [4]

$$h(t) = \sum_{k=0}^{N} \beta_k \exp(j\theta_k)\delta(t - \tau_k). \quad (1)$$

Here, k is the path index, β_k is the path gain, θ_k is the phase shift and τ_k is the time delay of the kth path. $\delta(\cdot)$ is the Dirac delta function.

The total number of paths is $N + 1$. Because the absolute delay of the channel is not important, the first arriving path is taken as time reference by setting $\tau_0 = 0$. Another way to represent the channel response is in the frequency domain, by taking the Fourier transform $H(f) = \mathcal{F}\{h(t)\}$. In the case of changing environment due to movement of transmitter, receiver, or people moving around, the parameters β_k, θ_k, and τ_k are functions of time. However, in this paper the channel is assumed to be quasi static. This assumption is reasonable when transmitter and receiver have a fixed position. To determine the characteristics of wideband channels, a wideband modulated sounding signal has to be used, e.g., a narrow pulse. For a pulselike signal the transmitted sounding signal is given as $s(t) = p(t)\cos(\omega_c t + \phi)$ where ω_c indicates the carrier frequency, ϕ the carrier phase, and $p(t)$ is pulse signal. For $\phi = 0$, the received signal is given by

$$\begin{aligned} r(t) &= \Re\{s(t)^* h(t)\} \\ &= \sum_{k=0}^{N} \beta_k p(t - \tau_k)\cos(\omega_c(t - \tau_k) + \theta_k). \end{aligned} \quad (2)$$

The pulse width or the measurement bandwidth determine the time resolution that can be achieved. The channel parameters, namely, power delay profile (PDP), path loss as a function of distance, coherence bandwidth, and delay spread τ_{rms}, are defined as follows.

A. Power Delay Profile

The PDP $P(t)$ gives the time distribution of the received signal power from a transmitted δ-pulse, and is defined as

$$P(t) \hat{=} h(t)h^*(t) = |h(t)|^2 = \sum_{k=1}^{N} \beta_k^2 \delta(t - \tau_k). \quad (3)$$

In practical measurements, the transmitted pulses $p(t)$ have finite width. When the pulse width of $p(t)$ is less than the delay time differences between the paths, the PDP is given by

$$P(t) = |r(t)| = \sum_{k=1}^{N} \beta_k^2 |p(t - \tau_k)|^2. \quad (4)$$

B. Path Loss

Different models have been presented for the path loss in an indoor environment. The following simple model is frequently used to describe path loss [5], [6]

$$\text{Loss} = S_0 + 10a\log_{10}(d/d_0) \quad (5)$$

where a is the power loss exponent of the environment and d [m] is the distance between the transmit and receive antennae. S_0 is the free space loss of a path of d_0 meter. Often $d_0 = 1$ m is chosen. When this parameter is measured with the antenna in the far field region, also the antenna gains are taken into account in the model.

C. RMS Delay Spread

The rms delay spread τ_{rms} is a measure for the amount of signal dispersion [15]. τ_{rms} is defined as

$$\tau_{\text{rms}} = \sqrt{\int_{-\infty}^{\infty} (t - \tau_m)^2 P_{\text{norm}}(t)\, dt} \quad (6)$$

where τ_m is the mean excess delay time defined as $\tau_m = \int_{-\infty}^{\infty} tP_{\text{norm}}(t)\, dt$, and $P_{\text{norm}}(t)$ is the normalized PDP: $P_{\text{norm}}(t) = P(t)/P_{\text{tot}}$, with $P_{\text{tot}} = \int_{-\infty}^{\infty} P(t)\, dt$.

In the literature τ_{rms} is used to give a rough indication of the maximum data rate which can be reliably supported by the channel, when no special precaution are taken, like equalization or diversity techniques. The estimate of the maximum reliable data rate R_{max} is given by [16]

$$R_{\text{max}} = 1/4\tau_{\text{rms}}. \quad (7)$$

D. Coherence Bandwidth

The coherence bandwidth B_{coh}, is the statistical average bandwidth of the radio channel, over which signal propagation characteristics are correlated. The definition of the coherence bandwidth B_{coh} is based on the complex autocorrelation function $|R(\Delta f)|$ of the frequency response $H(f)$. $R(\Delta f)$ is defined as [7]

$$R(\Delta f) \hat{=} \int_{-\infty}^{\infty} H(f)H^*(f + \Delta f)\, df. \quad (8)$$

B_{coh} is now defined as the value of Δf where $|R(\Delta f)|$ has decreased with 3 dB. B_{coh} and τ_{rms} are related as $B_{\text{coh}} = 1/\alpha\tau_{\text{rms}}$ [17], [18], where is α constant. In case the PDP is exponentially distributed, $\alpha = 2\pi$ [18]. However, in practical situations the value of α is not a constant, it depends on the impulse response. From results presented in [7], [8], [16] values of α between 5–7 were found.

III. Propagation Measurements

This section describes the measurement principle, setup, locations, and results.

A. Measurement Principle

Instead of transmitting a narrow pulse width signal in the time domain, the measurement technique applied here is a wideband coherent frequency response measurement, which consists of coherent amplitude/phase measurements at 801 equidistant frequency points in a selected frequency band. Thus actually complex samples of $H(f)$ are taken in the frequency domain. The sampled frequency response of the multipath radio channel is converted into the impulse response in the time domain by taking the inverse Fourier transform.

The important measurement parameters are as follows.

1) The measurement bandwidth over which the samples are taken, $BW_{\text{meas}} = f_{\text{max}} - f_{\text{min}}$. BW_{meas} determines the

TABLE I
MEASUREMENT PARAMETERS

Frequency	BW_{meas}	τ_{res}	τ_{unamb}	R_{unamb}
2.4 GHz	0.5 GHz	3 ns	1.6 μs	480 m
4.75 GHz	0.5 GHz	3 ns	1.6 μs	480 m
11.5 GHz	1.0 GHz	1.5 ns	0.8 μs	240 m

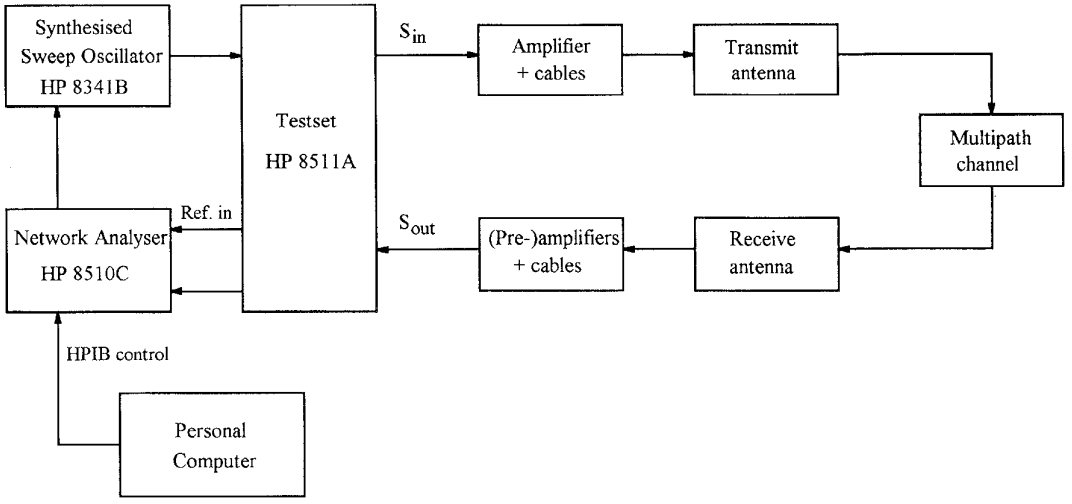

Fig. 1. Measurement system setup for wideband indoor measurements.

time resolution $\tau_{\rm res}$, that can be achieved in the time domain. The relation between $BW_{\rm meas}$ and $\tau_{\rm res}$ is given by

$$\tau_{\rm res} \approx \frac{1}{BW_{\rm meas}}. \tag{9}$$

2) The frequency distance between successive sample points $\Delta f_{\rm meas}$ determines the unambiguity in range and delay time. The unambiguous range of the measurements is the range [m] or delay [s] over which the received energy can be unambiguously related to a certain transmitted pulse. For larger distances, aliasing due to under sampling in the frequency domain will occur. The unambiguous range $R_{\rm unamb}$ is given by

$$R_{\rm unamb} = \frac{c}{\Delta f_{\rm samp}} \ [\rm m] \tag{10}$$

where c is the speed of light. The unambiguous time $\tau_{\rm unamb}$ is given by

$$\tau_{\rm unamb} = \frac{1}{\Delta f_{\rm samp}} \ [\rm s]. \tag{11}$$

3) Influence of the processing window. Before transformation of the measured frequency response to the impulse response in the time domain, the samples are weighted in order to suppress undesired sidelobes at the cost of a slightly decreased resolution. For this weighting, the Hanning window function was chosen, which is a good compromise between main peak width and sidelobe suppression. The Hanning window causes peak width widening by a factor 1.5. The parameters applying to the measurements performed at the frequencies 2.4, 4.75, and 11.5 GHz, are given in Table I.

B. Measurement Setup

The measurements are performed using an HP 8510C network analyzer. The measurement system is depicted in Fig. 1. Biconical antennae have been selected because of their large bandwidth and constant impedance over a large frequency band. These antennae have an omnidirectional radiation pattern in azimuth, and vertical polarization. Different antennae were dimensioned for each frequency band with equal gains of 2.5 dB, and equal beam width in the vertical plane of about 100°. Sucoflex 106A type cables were used to connect the antennae, amplifiers and HP8511A test set. The measurement system has been dimensioned in such a way that the signal-to-noise ratio (SNR) at the test set was not less than 20 dB. The distance between transmit and receive antenna was maximum 30 m. The maximum acceptable path loss was 123 dB, 139 dB, and 123 dB at 2.4, 4.75, and 11.5 GHz, respectively.

Before the measurements are carried out, the system is calibrated carefully at all three frequencies. Calibration is performed by disconnecting the antennae and connecting the transmitter output and receiver input by a calibrated attenuator at that point. The calibration results are used to compensate for the influence of phase and amplitude variations caused by the cables, amplifiers and measurement equipment. Note that the calibrated channel measurement results now contain the influence of the channel as well as both transmit and receive

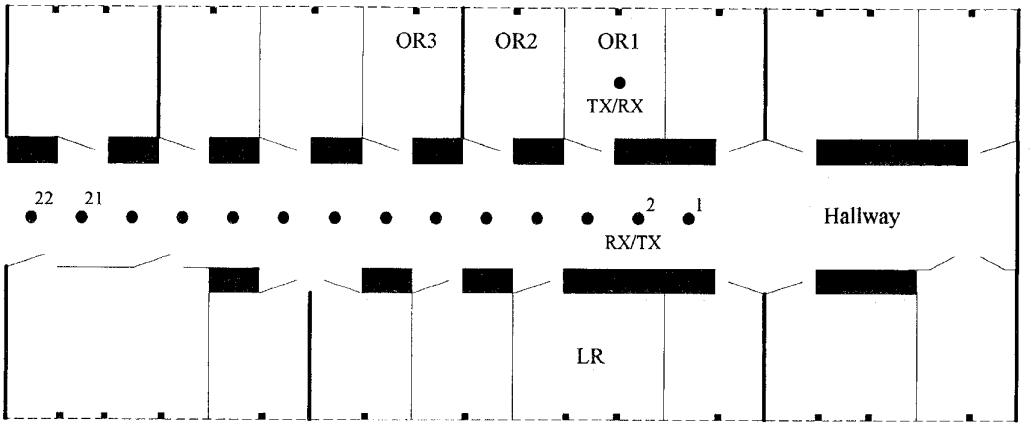

Fig. 2. Schematic overview of the measurement locations.

TABLE II
DIMENSIONS OF THE ROOMS USED FOR MEASUREMENTS

Location	Length	Width	Height
LR:	5.4 m	5.0 m	3.5 m
OR1, 2, 3:	3.6m	5.0 m	3.5 m
CR:	27 m	10 m	3.5 m
HW:	35 m	3.0 m	3.5 m

antennae. The influence of the antenna gain variations over the frequency band are so small that they can be neglected. Experiments showed that movement of cable after calibration had negligible effect on the measurements.

C. Description of Environment and Measurements

The measurements have been performed in a laboratory/office environment on the top floor of a three story building. The walls in this building are of brick/stone and plasterboard, and the floors are made of concrete. The glass in the windows in the rooms is not metal coated. The measurements were performed at four types of locations: one laboratory room (indicated as LR), three office rooms (indicated as OR1, OR2, and OR3), one conference room (indicated as CR) and in a hallway (indicated as HW). The locations of the rooms (except for CR) are shown in Fig. 2. The dimensions of the rooms are given in Table II.

The rooms OR1 and OR2 are separated by a plasterboard wall, OR2 and OR3 are separated by a brick wall. The CR room was subdivided by an RF permeable wall. In all rooms one side consists of windows. In LR, measurements were performed on ten receiver (RX) positions, with one transmitter (TR) position as shown in Fig. 3; seven positions had direct LOS, three had OBS. In OR1, OR2, and OR3, transmitter and receiver were in different rooms, all measurements were OBS. In CR, there were ten receiver positions (five LOS and five OBS) with one transmitter position. In HW, 22 positions as shown in Fig. 2, were chosen with 1 m separation, with the transmitter/receiver located in OR1, so nearly all positions were OBS. In LR also the influence of people being present in the room, was investigated and compared to the results for the empty room.

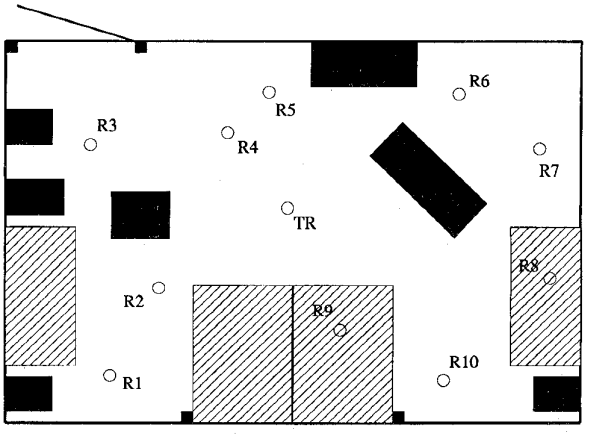

Fig. 3. Schematic overview of the measurement positions in LR room.

At every measurement position, except for the positions in HW, a cluster of measurements has been conducted at all three frequencies. A cluster consists of six positions, which are located on a circle with 12.5 cm diameter. The minimum distance between two positions on the circle is $\lambda/2$ at 2.4 GHz, λ at 4.75 GHz and 2λ at 11.5 GHz. The position of a cluster was fixed for all three frequencies, so that the results can be compared. The receiver antenna height was taken 1.5 m. The transmitter antenna height was taken to be 1.5 m and 3 m. During the time that is required to measure the channel, special precautions have been taken to keep the channel as static as possible.

D. Measurement Results

In Fig. 4, the measured PDP's are given for all three frequencies at the same position for an OBS path between OR1 and OR3. For short delays some paths can be matched at different frequencies, however for longer delays the PDP's are quite different. In Fig. 5, the frequency response at 2.4 GHz for the same position is given which shows a highly frequency selective channel. Fig. 6 shows the PDP and the average PDP of a cluster in LR for a LOS channel. It

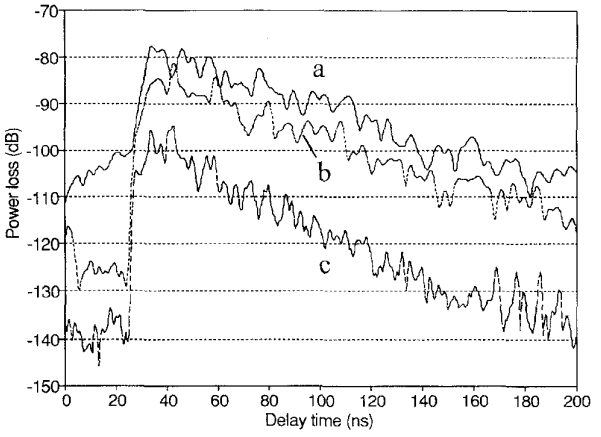

Fig. 4. PDP's in an OBS situation of a channel between OR1 and OR3, with (a) 2.4 GHz, (b) 4.75 GHz, and (c) 11.5 GHz.

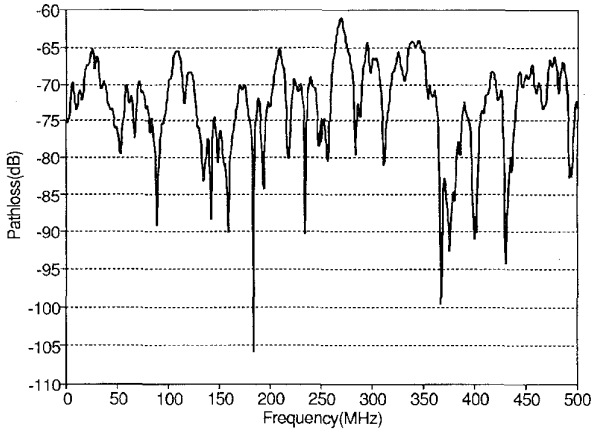

Fig. 5. Frequency response at 2.4 GHz for the same channel between OR1 and OR2 as shown in Fig. 4.

is clear that the PDP's of a cluster do not show great differences when the measurement position is changed over a few wavelengths.

1) Path Loss: The path loss has been computed as the average power loss over the measured frequency band (0.5 GHz bandwidth at 2.4 and 4.75 GHz and 1 GHz at 11.5 GHz). The path loss as function of distance at the three frequencies is treated separately for LOS and OBS situations. In Figs. 7 and 8, the path loss results are shown as a function of the distance for LOS and OBS channels, respectively. From the results the path loss law has been determined by fitting a straight line through the attenuation-distance scatter plot. The simple model that comes with this regression is described by a modified version of (5)

$$\text{Loss} = S_0 + 10a\log_{10}(d) + b \tag{12}$$

where S_0 is the path loss at 1 m distance, a is the path loss exponent, d is the distance between transmitter and receiver in [m] and b is the value of the regression line at $d = 1$ m. The measured value of S_0 is 43.1 dB, 48.4 dB, and 57.6 dB at 2.4, 4.75, and 11.5 GHz, respectively. In Table III, the values for

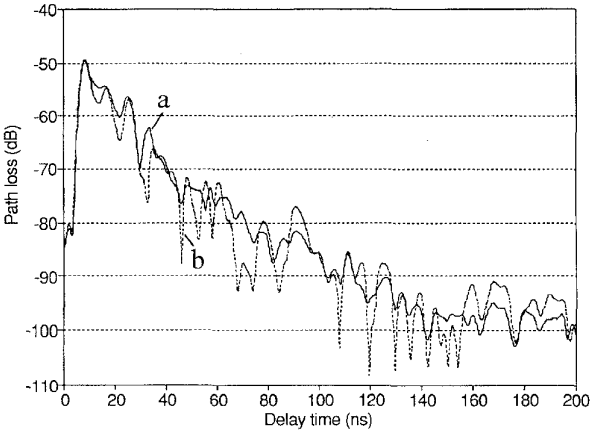

Fig. 6. PDP for a LOS channel (receiver position 1) in room LR, with (a) averaged PDP over six cluster positions, (b) one specific PDP of that cluster.

a, b and σ_L (the rms error of the measured values with respect to the regression line) are given for LOS and OBS situations.

For LOS situations the path loss exponent value is very close to the expected value for free-space propagation $a = 2$, at all three frequencies. This was to be expected, because the channel response is dominated by the direct LOS path. The values for b are slightly negative, but close to 0 dB. The rms error σ_L is small (<2.5 dB), however, increases with frequency.

For OBS situations the path loss exponent value a increases with increasing frequency. The calculated values for b are becoming increasingly negative with increasing frequency. Also the rms error σ_L increases with frequency. From these results it can be concluded that the simple model used here, performs well in LOS situations, but is not accurate for OBS paths. More complicated models, which take into account attenuation jumps caused by walls and other obstructions, are proposed in [5], [6].

2) Influence of People: In the laboratory room LR, measurements have been conducted to investigate the influence of people located at different positions in the room, on the transmission channel. The measurements have been performed for one single radio channel (transmitter-receiver set-up TR-R10 in Fig. 3) and ten different people configuration (five LOS and five OBS: when people obstruct the direct path). For every frequency the peoples locations were also different. Two transmitter antenna heights were used: 1.5 and 3 m. The path loss results with people are compared with the results for the empty room. The excess attenuation that was found, is given in table 4. These results show that the presence of people in the LOS case only slightly influences the received power level (less than 1 dB). Obstruction of the direct path has a clear negative effect. For the transmitter antenna at 1.5 m the excess attenuation is 4–5.5 dB, for the antenna at 3 m the excess attenuation was found to be less: 1.5–3.5 dB. For both situations LOS and OBS, no clear difference in behavior between the three frequencies was found. One should be careful with drawing general conclusions from these results since they were derived from a very limited number of measurements at only one location.

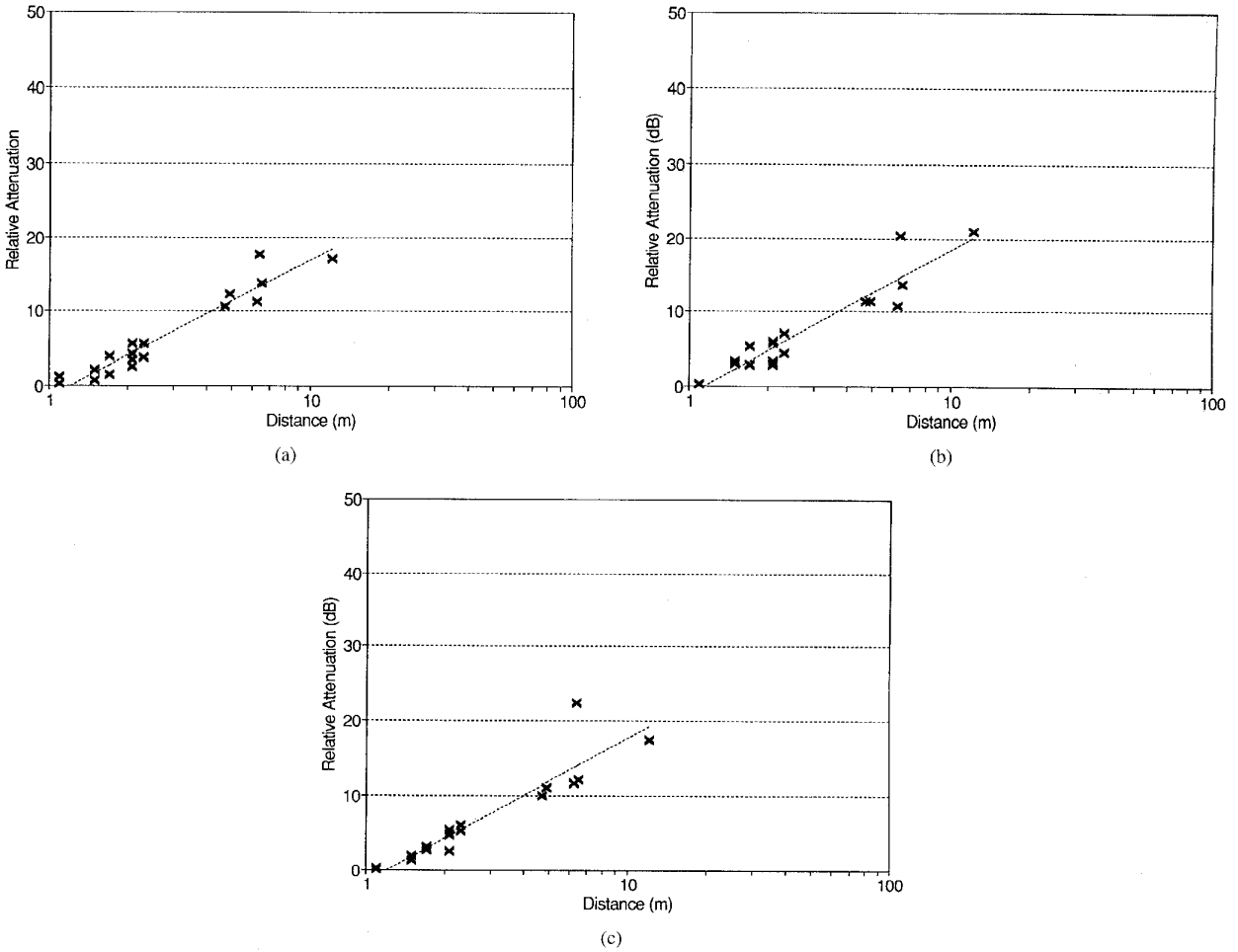

Fig. 7. Attenuation as a function of the distance for LOS at: (a) 2.4 GHz; (b) 4.75 GHz; (c) 11.5 GHz.

3) The rms Delay Spread: The rms delay spread τ_{rms}, as defined in (6), is a measure for the dispersion of the radio channel, and can therefore be used to estimate the maximum usable symbol rate. For all measured channel responses, τ_{rms} has been calculated. The average values and standard deviation of τ_{rms} at 2.4, 4.75, and 11.5 GHz are given for different locations and for two transmitter antenna heights in Tables V and VI, for the LOS and OBS situations, respectively.

From these results it is concluded that the average $\overline{\tau}_{\mathrm{rms}}$ is minimum at 11.5 GHz for all LOS as well as in most OBS channels. The values of τ_{rms} at 11.5 GHz are on the average 30% less than at 2.4 and 4.75 GHz. In LOS channels the height of the transmitter antenna only slightly affects $\overline{\tau}_{\mathrm{rms}}$. However, reducing the antenna height in OBS channels yields an increase of both $\overline{\tau}_{\mathrm{rms}}$ and σ_{rms}. In the larger rooms (e.g. CR and HW) large τ_{rms} values are found due to the large distances between reflective walls and objects. Also the variation $\sigma_{\tau_{\mathrm{rms}}}$ is large at these locations. However, this observation is not always true for LOS channels. When transmitter and receiver are in adjacent rooms (OR1 $\rightarrow$ OR2), τ_{rms} is less compared to the situation when there is an empty room in between (OR1 $\rightarrow$ OR3). The presence of people in the laboratory room LR do not show a significant effect on τ_{rms}, even not in case the direct path is obstructed.

During the measurements antennae with a wide opening angle were used. This leads to relatively low τ_{rms} values compared to cases with high directive omnidirectional antennae [19]. The variation of τ_{rms} within a cluster is very small, usually less that 10% of the average value. In Fig. 9, the variations in τ_{rms} are shown for the different locations by means of the cumulative distribution functions of τ_{rms} at the three frequencies. In general the values for τ_{rms} are less than 30 ns. This however, is not true for the measurements done in HW. In Figs. 10 and 11 the results for τ_{rms} as a function of the distance between transmitter and receiver are given, for the cases that the transmitter is in an office room (OR1) and the receiver is in HW and vice versa. These results show that the variation of τ_{rms} in HW is large. τ_{rms} seems to increase with the distance between transmitter and receiver. Excessively large values in the order of 70 ns were observed on some positions at about the middle of the hall way. The measurements with the receiver in HW show larger τ_{rms} than with the transmitter placed in the HW. This illustrates clearly that the environment of the receiver has large impact on τ_{rms}.

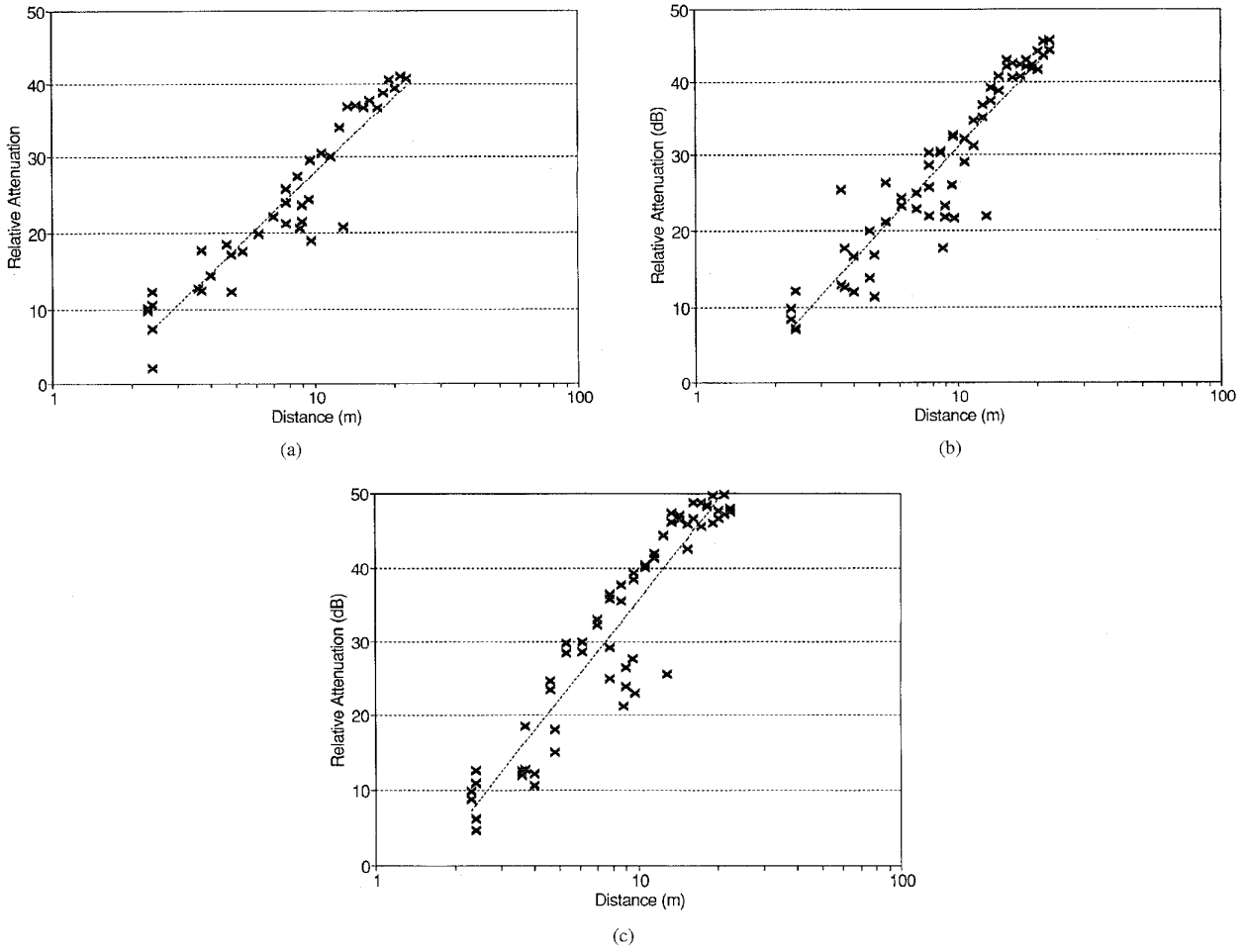

Fig. 8. Attenuation as a function of the distance for OBS at: (a) 2.4 GHz, (b) 4.75 GHz, and (c) 11.5 GHz.

TABLE III
CALCULATED RESULTS OF THE PATH LOSS VARIABLES a, b AND THE RMS ERROR AT 2.4, 4.75, AND 11.5 GHz

Frequency	Location	a	b [dB]	σ_L [dB]
2.4 GHz	LOS	1.86	-1.6	1.6
	OBS	3.33	-5.4	3.6
4.75 GHz	LOS	1.98	-1.2	2.0
	OBS	3.75	-6.5	4.1
11.5 GHz	LOS	1.94	-1.7	2.3
	OBS	4.46	-8.9	5.0

4) Coherence Bandwidth: The coherence bandwidth B_{coh} is defined as given by (8). It was found that the shape of the frequency correlation function strongly depends on the characteristics of the multipath channel. The B_{coh} results show a large variance in most of the situations, also within a cluster. In many LOS situations the correlation level did not drop below the $-$ 3 dB level for a bandwidth of over 250 MHz. This effect was seen for about 30% of the measurements in the office room at the three frequencies. In the conference room this percentage was much less (about 6%). A remarkable observation is that for the lower frequencies about 40% of the clusters had at least one position with $B_{\text{coh}} >$ 250 MHz. At 11.5 GHz this percentage was even 65%.

The cumulative distribution functions for B_{coh} have been calculated from all measured LOS and OBS channels, and are shown in Figs. 12 and 13. It is found that for LOS situations more than 27% of the positions have B_{coh} of over 250 MHz. For OBS situations this percentage is much less

TABLE IV
EXCESS ATTENUATION AND VARIANCE FOR THE LR ROOM WITH PEOPLE BEING PRESENT, COMPARED TO THE EMPTY LR ROOM, AT 2.4, 4.75 AND 11.5 GHz

Frequency	Location	Antenne height	Avg. excess attenuation (dB)	σ (dB)
2.4 GHz	LOS	1.5 m	-0.33	0.3
		3.0 m	0.24	0.3
	OBS	1.5 m	4.84	1.8
		3.0 m	2.73	2.3
4.75 GHz	LOS	1.5 m	0.64	1.1
		3.0 m	-0.3	0.8
	OBS	1.5 m	5.35	3.7
		3.0 m	1.46	1.4
11.5 GHz	LOS	1.5 m	0.19	0.6
		3.0 m	0.28	0.8
	OBS	1.5 m	4.33	1.5
		3.0 m	3.59	0.6

TABLE V
RMS DELAY SPREAD (MEAN AND STANDARD DEVIATION) FOR LOS CHANNELS IN DIFFERENT TYPES OF ROOMS AND FOR TRANSMITTER ANTENNA HEIGHT OF 1.5 m AND 3 m

Location	2.4 GHz				4.75 GHz				11.5 GHz			
	$\bar{\tau}_{rms}$ (ns)		$\sigma_{\tau_{rms}}$ (ns)		$\bar{\tau}_{rms}$ (ns)		$\sigma_{\tau_{rms}}$ (ns)		$\bar{\tau}_{rms}$ (ns)		$\sigma_{\tau_{rms}}$ (ns)	
Antenna height	1.5m	3m	1.5m	3m	1.5m	3m	1.5m	3m	1.5m	3m	1.5m	3m
LR	8.0	7.3	2.2	1.4	8.5	8.5	1.4	2.4	6.2	4.6	0.9	1.3
LR people	7.4	8.3	1.6	0.5	7.9	11.8	1.2	1.0	5.1	5.6	0.4	0.5
CR	-	14.9	-	2.9	-	18.0	-	5.2	-	12.8	-	3.7
HW	-	5.4	-	0.9	-	10.2	-	2.6	-	4.3	-	1.4

TABLE VI
RMS DELAY SPREAD (MEAN AND STANDARD DEVIATION) FOR OBS CHANNELS IN DIFFERENT TYPES OF ROOMS AND FOR TRANSMITTER ANTENNA HEIGHT OF 1.5 m AND 3 m

Location	2.4 GHz				4.75 GHz				11.5 GHz			
	$\bar{\tau}_{rms}$ (ns)		$\sigma_{\tau_{rms}}$ (ns)		$\bar{\tau}_{rms}$ (ns)		$\sigma_{\tau_{rms}}$ (ns)		$\bar{\tau}_{rms}$ (ns)		$\sigma_{\tau_{rms}}$ (ns)	
Antenna height	1.5m	3m	1.5m	3m	1.5m	3m	1.5m	3m	1.5m	3m	1.5m	3m
LR	17.4	12.4	7.2	2.5	12.4	11.6	2.5	2.3	7.9	6.5	2.1	1.2
LR people	10.8	8.8	3.1	1.1	10.6	11.1	1.1	1.2	5.4	5.4	0.9	1.1
OR1→ OR2	19.8	12.1	1.4	1.1	21.2	12.6	2.9	1.1	14.4	9.7	1.1	1.6
OR1→ OR3	23.1	19.2	1.7	3.0	21.5	19.3	1.3	1.9	13.6	12.4	1.8	1.5
CR	-	21.1	-	5.5	-	23.6	-	4.3	-	20.1	-	2.9
HW	-	21.6	-	17.0	-	15.2	-	4.4	-	18.6	-	10.1

(5%). The relation $\alpha = 1(\tau_{\mathrm{rms}} \cdot B_{\mathrm{coh}})$, has been evaluated for the measured results. In Fig. 14, the cumulative distribution functions of α are given separately for LOS and OBS situations for the three frequencies. The median values of α found for LOS and OBS are about four and five, respectively, which is in agreement with the results given in [17], [18].

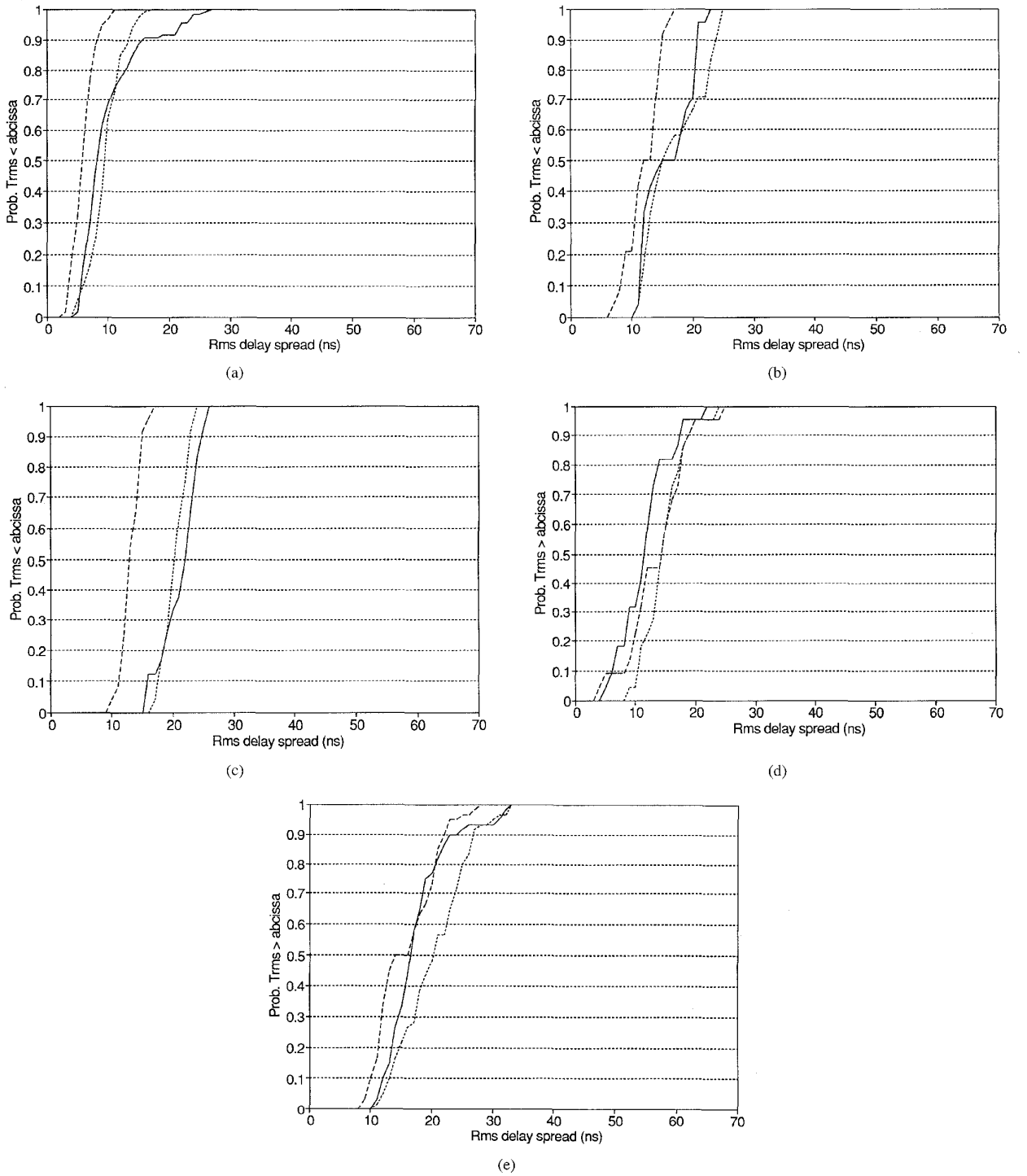

Fig. 9. CDF of τ_{rms} with transmitter and receiver in: (a) LR room, (b) adjacent rooms OR1 $\leftrightarrow$ OR2, (c) rooms OR1 $\leftrightarrow$ OR3, (d) CR room, (e) with transmitter in the HW and receiver in OR1 where the frequency band is indicated by: ___: 2.4 GHz; · · · · · ·: 4.75 GHz; - - - -: 11.5 GHz.

IV. Analytical Model for BER Evaluation

This section describes the analytical approach to evaluate the BER of a BPSK modulated signal in a stationary frequency selective multipath channel, using a coherent BPSK receiver [21], [22]. The complex channel impulse response variables β_k, θ_k, and τ_k are used in the model for the BER calculations. Therefore, the measured channel impulse response, which has a continuous character, is transformed to the discrete channel response variables β_k, θ_k, and τ_k, which are the amplitude, phase, and time delay at the local maximums

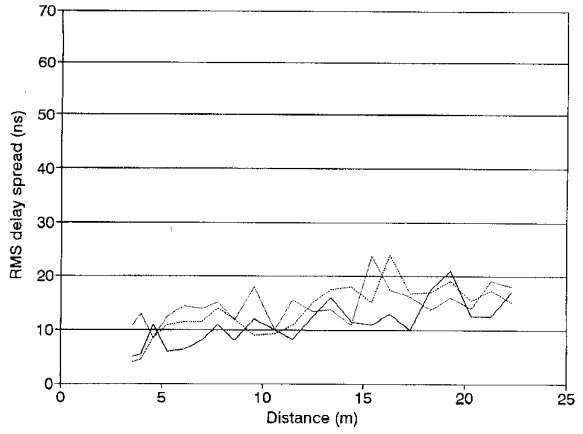

Fig. 10. $\tau_{\rm rms}$ verses distance with transmitter in HW and receiver in OR1, at: ___: 2.4 GHz; · · · · · ·: 4.75 GHz; ----: 11.5 GHz.

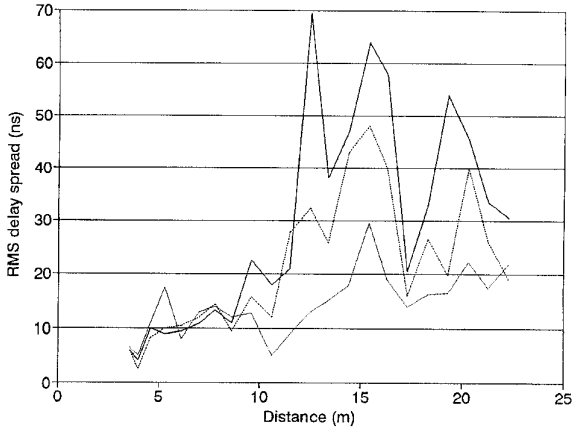

Fig. 11. $\tau_{\rm rms}$ verses distance with transmitter in OR1 and receiver in HW, at: ___: 2.4 GHz; · · · · · ·: 4.75 GHz; ----: 11.5 GHz.

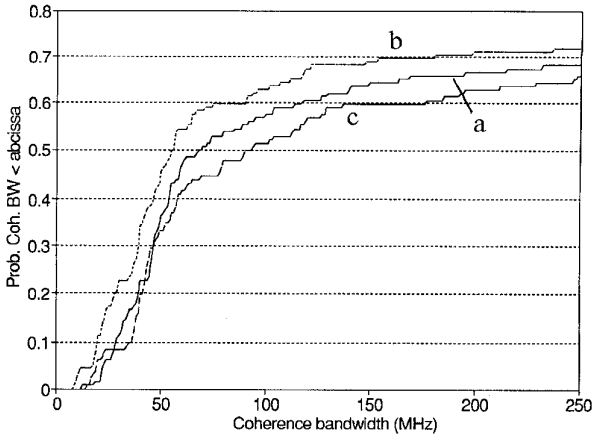

Fig. 12. CDF of the coherence bandwidth for LOS channels: (a) 2.4 GHz, (b) 4.75 GHz, and (c) 11.5 GHz.

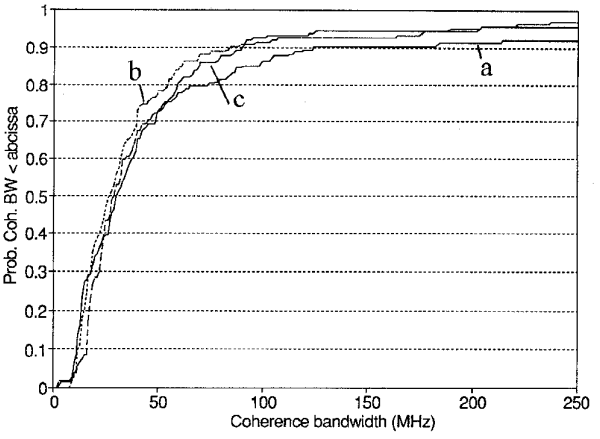

Fig. 13. CDF of the coherence bandwidth for OBS channels: (a) 2.4 GHz, (b) 4.75 GHz, and (c) 11.5 GHz.

of the response. These maximums are identified as discrete paths.

A. Signal Model

The complex equivalent baseband representation of a BPSK modulated signal is written as

$$\overline{s}_B(t) = \sqrt{P}\, d(t) \exp(j\phi) \tag{13}$$

where P denotes signal power, and ϕ indicates carrier phase. The overbar denotes a complex signal. The real modulated signal is given by

$$s(t) = \Re\{\sqrt{2}\overline{s}_B(t) \exp(j\omega_c t)\} = \sqrt{2P}\, d(t) \cos(\omega_c t + \phi) \tag{14}$$

where ω_c is carrier frequency, and $\Re\{z\}$ denotes the real part of the complex value z. Without loss of generality we will assume that $\phi = 0$. $d(t)$ is a random data signal which consists of rectangular pulses with duration T, and is given by

$$d(t) = \sum_{k=0}^{\infty} a_k \Pi(t - kT) \tag{15}$$

where $a_k \in \{-1, +1\}$ with equal probability of occurrence. When $s(t)$ reaches the receiver via a multipath channel with impulse response $h(t)$ as given by (1), the equivalent baseband received signal $r_B(t)$ is

$$r_B(t) = \Re\{\overline{s_B}(t)^* h(t)\} = \sqrt{P} \sum_{k=0}^{N} \beta_k\, d(t - \tau_k) \cos\theta_k \tag{16}$$

and the real received signal is

$$r(t) = \Re\{\sqrt{2}\overline{r}_B(t) \exp(j\omega_c t)\}. \tag{17}$$

B. BPSK Receiver Model

In the model a conventional coherent BPSK receiver, matched to the AWGN channel, is used. The reference carrier is recovered from the received signal by means of a squaring loop, [20]. A block diagram of the receiver and the squaring loop carrier recovery circuit is shown in Fig. 15. The bandwidth of the phase locked loop (PLL) of the carrier recovery circuit is assumed to be very small compared to the bitrate, so that phase-jitter due to AWGN and intersymbol interference (ISI), caused by multipath signals,

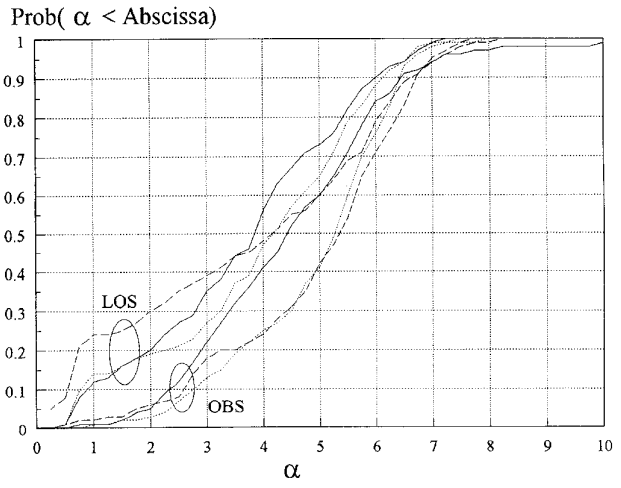

Fig. 14. CDF of $\alpha = 1/(\tau_{\rm rms} \cdot B_{\rm coh})$ for LOS and OBS channels ___: 2.4 GHz; · · · · ·: 4.75 GHz; - - - -: 11.5 GHz.

can be neglected. The recovered carrier phase for the multipath channel is determined from

$$\bar{r}_B^2(t) = P \sum_{i=0}^{N} \sum_{j=0}^{N} \beta_i \beta_j \, d(t-\tau_j) \exp\left(j(\theta_i + \theta_j)\right) \qquad (18)$$

which is the complex baseband equivalent signal of the signal component at $2f_c$ after squaring of the real signal $r(t)$. The PLL locks on this component at $2f_c$, whereas the low-pass signal is filtered out. In the ideal case that the PLL-bandwidth $\rightarrow 0$, the recovered phase is given by

$$\begin{aligned}\phi_c &= \tfrac{1}{2} \arg\left\{E[\bar{r}_B^2(t)]\right\} + n\pi \\ &= \tfrac{1}{2} \arg\left\{ E\left[P \sum_{i=0}^{N} \sum_{j=0}^{N} \beta_i \beta_j \, d(t-\tau_i)\, d(t-\tau_j) \right.\right. \\ &\qquad \left.\left. \cdot \exp\left(j(\theta_i + \theta_j)\right) \right] \right\} + n\pi \\ &= \tfrac{1}{2} \arg\left\{ \sum_{i=0}^{N} \sum_{j=0}^{N} \beta_i \beta_j R_d(\tau_i - \tau_j) \exp\left(j(\theta_i + \theta_j)\right) \right\} \\ &\qquad + n\pi \qquad (19a)\end{aligned}$$

where $R_d(\tau_i - \tau_j)$ is the autocorrelation function which value indicates the fraction of the bit time that two paths carry the same bit during a bit interval, with

$$\begin{aligned} R_d(\tau_i - \tau_j) &= 1 - \frac{|\tau_i - \tau_j|}{T} \quad \text{if } |\tau_i - \tau_j| \le T \\ &= 0 \qquad\qquad\qquad\quad \text{if } |\tau_i - \tau_j| > T. \qquad (19b)\end{aligned}$$

The uncertainty of $n\pi$ is caused by the phase ambiguity of the squaring loop circuit. This ambiguity requires the data signal to be differentially encoded.

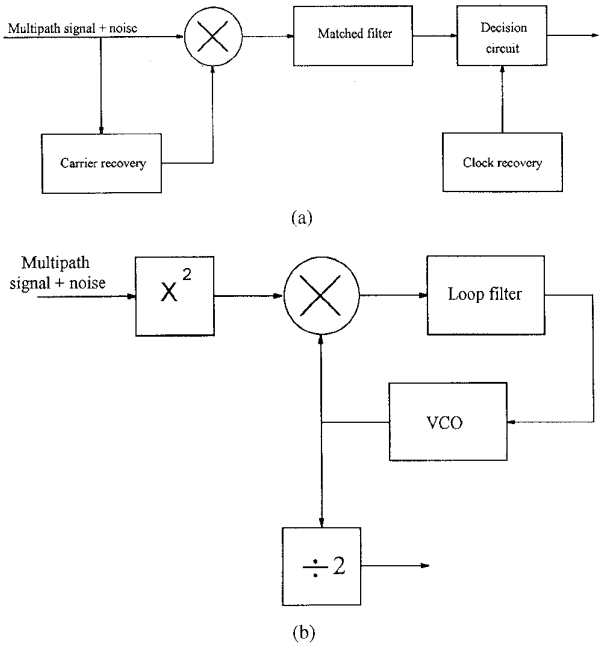

Fig. 15. Block diagram of (a) the coherent BPSK receiver and (b) the squaring loop carrier recovery circuit.

C. BER for a Stationary Frequency Selective Multipath Channel

The input signal of the matched filter is the baseband component which results after multiplication of the received signal $r(t)$ with the recovered reference carrier

$$\begin{aligned} r_{\rm dem}(t) &= r(t) \cos\left(\omega_c t + \phi_c\right) \\ &= \sqrt{P} \sum_{k=0}^{N} \beta_k \, d(t-\tau_k) \cos\left(\theta_k - \phi_c\right). \qquad (20)\end{aligned}$$

This signal is the sum of the contributions of all $N+1$ paths. The maximum number of bits which are active in the channel during one bit interval T is $L+2$ with, $L = \lceil (\tau_N - \tau_0)/T \rceil = \lceil \tau_N / T \rceil$, where $\lceil x \rceil$ indicates the integer value larger or equal to x.

Because the energy that is received during a bit time results from $L+2$ bits, it is necessary for the BER calculation to select a desired bit from the active bits in the channel, as the bit that will be detected by the receiver (see Fig. 15). The BER of the desired bit depends on the combination of receiver timing, received energy from that bit in the corresponding integration interval and the amount of ISI energy in that interval. Different criteria for selection of the desired bit and bit timing, can be used: 1) lowest BER for the desired bit; 2) largest contribution of the desired bit to the matched filter output signal; 3) maximum signal-to-intersymbol interference ratio (SIIR) for the desired bit; 4) maximum total energy at the matched filter output.

The received power for a single bit can be determined by transmitting a test bit over the multipath channel, as depicted in Fig. 16. Let the test bit be defined as $p_{\rm test}(t) \triangleq U(t) - U(t-T)$,

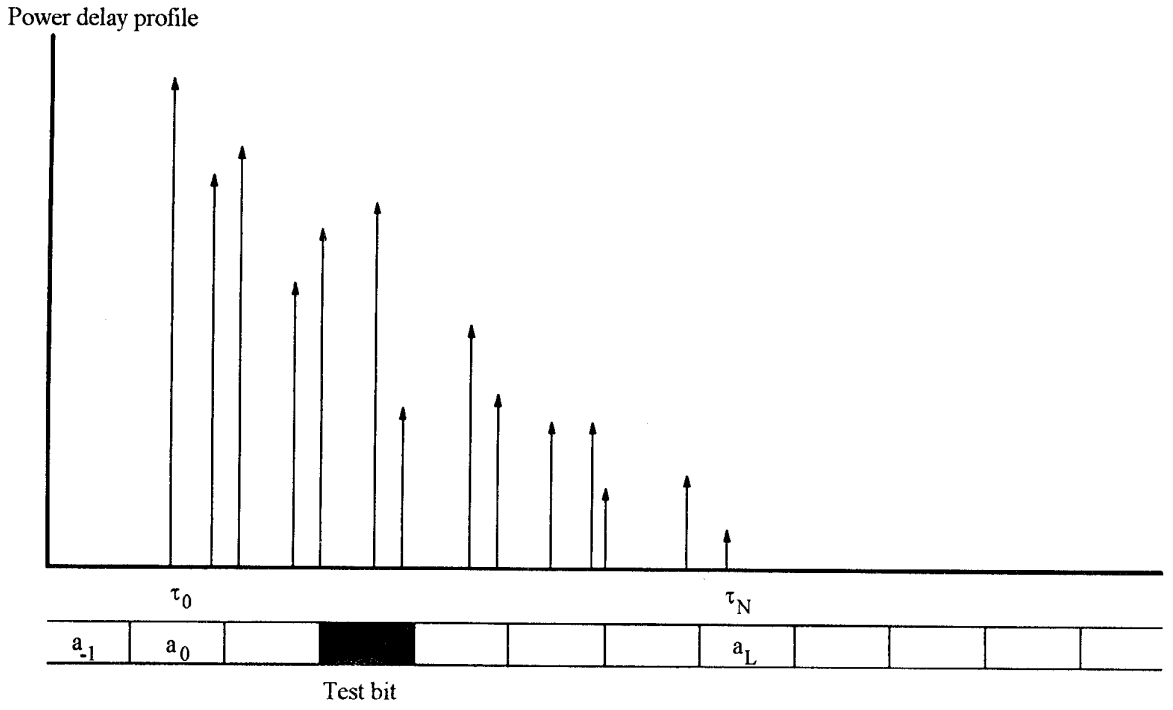

Fig. 16. Paths contributing to the received signal of a test bit, and the other active bits in a multipath channel.

then the equivalent received complex baseband signal is

$$r_{B\_\text{test}}(t) = \Re\{p_{\text{test}}(t)^* h(t)\} = \sum_{k=0}^{N} \beta_k p_{\text{test}}(t-\tau_k)\cos\theta_k. \tag{21}$$

The output signal $s_{\text{test}}(\tau_s)$ for the test bit for a given sample time τ_s, is given by

$$s_{\text{test}}(\tau_s) = \int_{\tau_s - T}^{\tau_s} \left[\sum_{k=0}^{N} \beta_k p_{\text{test}}(t-\tau_k)\cos(\theta_k - \phi_c)\right] dt. \tag{22}$$

τ_s is the sample time referred to the delay time of the paths in the channel impulse response $h(t), \tau_s \in [T, \tau_N + T]$. The sign of s_{test} is determined by the phases of the contributing paths. When a real data signal is transmitted, a sequence of bits is active. If we denote the desired bit a_d, the sequence of active bits can be written in vector notation as

$$\boldsymbol{a} = (a_{-1}, a_0, a_1, \cdots, a_{d-1}, a_d, a_{d+1}, \cdots, a_L)$$

with

$$a_j \in \{-1, +1\}.$$

The position of a_d in $\boldsymbol{a}$ depends on $h(t)$, and the selection criterion used to determine τ_s. The index d is equal to $d = \lceil \tau_s/T \rceil$. In the integration interval $[\tau_s - T, \tau_s)$ in general two bits, a_{i-1} and $a_i \in \boldsymbol{a}$, will be active in the kth path, where the index i is given by $i = \lceil \tau_k/T \rceil$. The contribution of path k to the output signal of the matched filter is now given by

$$\begin{aligned} s_k &= \sqrt{P}\beta_k T\cos(\theta_k - \phi_c)[(1-\Delta_k)a_{i-1} + \Delta_k a_i] \\ &= a_{i-1}\kappa_{k,i-1} + a_i\kappa_{k,i} \end{aligned} \tag{23}$$

with

$$\begin{aligned} \kappa_{k,i-1} &= \sqrt{P}\beta_k(1-\Delta_k)T\cos(\theta_k - \phi_c); \\ \kappa_{k,i} &= \sqrt{P}\beta_k\Delta_k T\cos(\theta_k - \phi_c). \end{aligned} \tag{24}$$

Δ_k indicates the fraction of bit a_i in the integration interval for path k

$$\begin{aligned} \Delta_k &= \text{Frac}\left(\frac{\tau_k - \tau_s}{T}\right) \quad \text{if } \tau_s < \tau_k \\ &= \text{Frac}\left(\frac{\tau_s - \tau_k}{T}\right) \quad \text{if } \tau_s > \tau_k. \end{aligned} \tag{25}$$

The total output signal of the matched filter for all $N+1$ path contributions is given by

$$s_{\text{out}}(\boldsymbol{a}, \tau_s) = \boldsymbol{a} \cdot K(\tau_s). \tag{26}$$

Here $K(\tau_s)$ is the path matrix for sample time τ_s. Note that $K(\tau)$ is periodic in T.

$$K = \begin{pmatrix} \kappa_{0,-1} & 0 & 0 & \cdots & 0 & 0 \\ \kappa_{0,0} & \kappa_{1,0} & \kappa_{2,0} & \cdots & \cdots & \cdots \\ 0 & \kappa_{1,1} & \kappa_{2,1} & \cdots & \cdots & \cdots \\ 0 & 0 & 0 & \cdots & \cdots & \cdots \\ \cdots & \cdots & \cdots & \cdots & \kappa_{N-1,L-2} & \cdots \\ \cdots & \cdots & \cdots & \cdots & \kappa_{N-1,L-1} & \kappa_{N,L-1} \\ 0 & 0 & 0 & \cdots & 0 & \kappa_{N,L} \end{pmatrix}. \tag{27}$$

The number of rows of K is equal to $L+2$, which is equal to the number of active bits in the channel during one bit time. Row l, with $l \in \{-1, 0, \ , L\}$, contains the contribution of bit a_l. The number of columns of K is $N+1$, which is equal to the number of paths, where

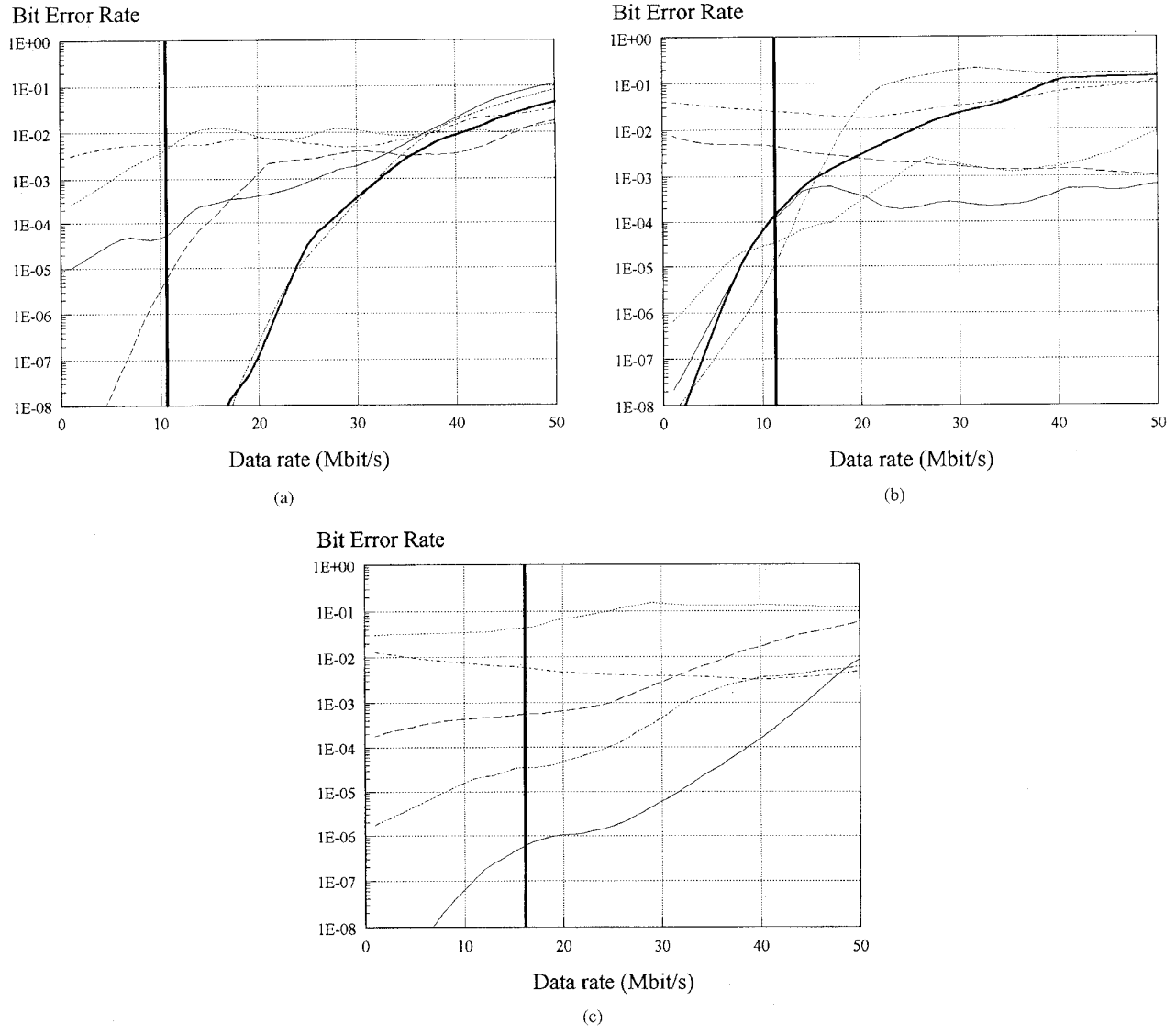

Fig. 17. BER as function of data rate in location OR1OR3, at: (a) 2.4 GHz; (b) 4.75 GHz; (c) 11.5 GHz. The different positions in the circular cluster are indicated as: 1: ____; 2: {–}{–}; 3: · · · · · ·; 4: · - · - · -; 5: ____; 6: ·· - ·· - · . The bold vertical line indicates $R_{\max} = 1/4\overline{\tau}_{\text{rms}}$.

column vectors K_k contain the contribution of path k. K_k is defined as $K_k \hat{=} (0, 0, \cdots, 0, \kappa_{k,i-1}, \kappa_{k,i}, 0, \cdots, 0)^T$, where superscript T indicates the transpose. Each column has only two successive nonzero elements, because only two bits are active during a bit time, and all preceding and following elements are zero. Now the received power from bit i, S_i, can be written as

$$S_i(\tau_s) = \left| \sum_{k=0}^{N} \kappa_{k,i}(\tau_s) \right|^2. \tag{28}$$

Let the desired bit have the fixed value $a_d = +1$, then vector $\boldsymbol{a}$ can take on $V = 2^{L+1}$ different values, each resulting in a different output signal $s_{\text{out}}(\boldsymbol{a}_z | a_d = +1)$, with $\boldsymbol{a}_z \in \{\boldsymbol{a}_1, \cdots, \boldsymbol{a}_V\}$. The probability of an error, $P_{ez}(\varepsilon)$ for $\boldsymbol{a_z}$ is given by

$$\begin{aligned} P_{ez} &= P(\varepsilon | a_d = +1, \boldsymbol{a}_z) = P(\text{sign})(s_{\text{out}}(\boldsymbol{a}_z | a_d = +1)) \\ &\quad = -\text{sign}\,(s_d)) \\ &= \begin{cases} Q\left(\dfrac{|s_{\text{out}}(\boldsymbol{a}_z | a_d = +1)|}{\sigma_n} \right) \\ \qquad \text{if sign}\,(s_{\text{out}}) = \text{sign}\,(s_d) \\ 1 - Q\left(\dfrac{|s_{\text{out}}(\boldsymbol{a}_z | a_d = +1)|}{\sigma_n} \right) \\ \qquad \text{if sign}\,(s_{\text{out}}) = -\text{sign}\,(s_d) \end{cases} \end{aligned} \tag{29}$$

with $Q(z) = \frac{1}{\sqrt{2\pi}} \int_z^\infty e^{-\lambda^2/2}\, d\lambda$ and σ_n^2 the received noise power. Sign (s_d) is determined with (22). The BER is calculated by averaging P_{ez} over all 2^{L+1} possible sequences $\boldsymbol{a_z}$

$$P_e(\varepsilon | a_d = +1) = \frac{1}{2^{L+1}} \sum_{z=1}^{2^{L+1}} P_{ez}. \tag{30}$$

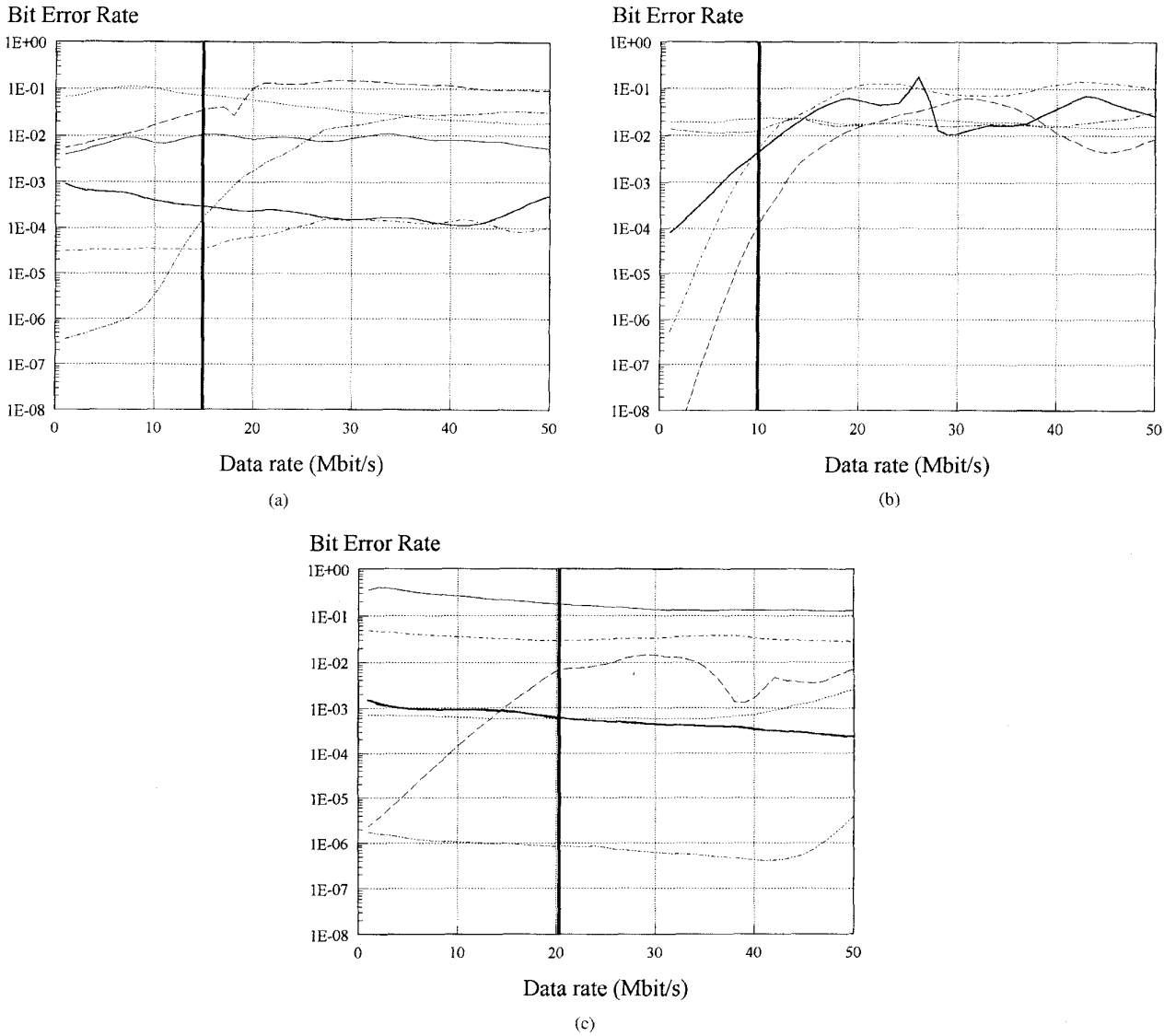

Fig. 18. BER as function of data rate in location CR (LOS), at: (a) 2.4 GHz; (b) 4.75 GHz; (c) 11.5 GHz. The different positions in the circular cluster are indicated as: 1: ____; 2: {–}{–}; 3: · · · · · ·; 4: -·-·-·-; 5: ____; 6: ····· . The bold vertical line indicates $R_{\max} = 1/4\overline{\tau}_{\rm rms}$.

σ_n^2 is related to the average SNR γ as $\sigma_n^2 = S_{\rm av}/\gamma$ with $S_{\rm av}$ is the average received signal power

$$S_{\rm av} = P\sum_{k=0}^{N}\beta_k^2. \tag{31}$$

Now τ_s is optimized to one of the criteria mentioned earlier. In the following we have selected optimum timing τ_s for minimum BER. Therefore, the BER results given here are a lower bound. The optimum timing is calculated by evaluation of the BER when the sample time τ_s is varied with small steps over the bit duration T (note that the path matrix is periodic with T). At every τ_s the BER is calculated for the desired bit, which has maximum energy as determined with (28).

D. BER Results for Measured Indoor Channels

For a number of measured clusters as described in Section III, the BER has been calculated as function of the bit rate at 2.4, 4.75, and 11.5 GHz. In the calculations only paths which are less than 30 dB down compared to the dominant path are assumed to give a significant contribution to the received signal. Weaker paths are neglected, which makes computations less time consuming. The SNR was taken $\gamma = 10$ dB. Instead of $S_{\rm av}$, the average power $S_{\rm avc}$ over six positions in the cluster has been used as reference signal power to determine σ_n^2: $\sigma_n^2 = S_{\rm avc}/\gamma$. $S_{\rm avc}$ is given by

$$S_{\rm avc} = \frac{P}{6}\sum_{j=1}^{6}\sum_{k=1}^{N_j}\beta_{j,k}^2 \tag{32}$$

where j indicates the cluster position, $j = \{1, \cdots, 6\}$ and N_j is the number of relevant paths for position j. In Figs. 17–19, BER results as a function of the bit rate are shown for 2.4, 4.75, and 11.5 GHz, for three cluster at the following positions: OR1 → OR2 (OBS), CR (LOS), and CR (OBS). The vertical

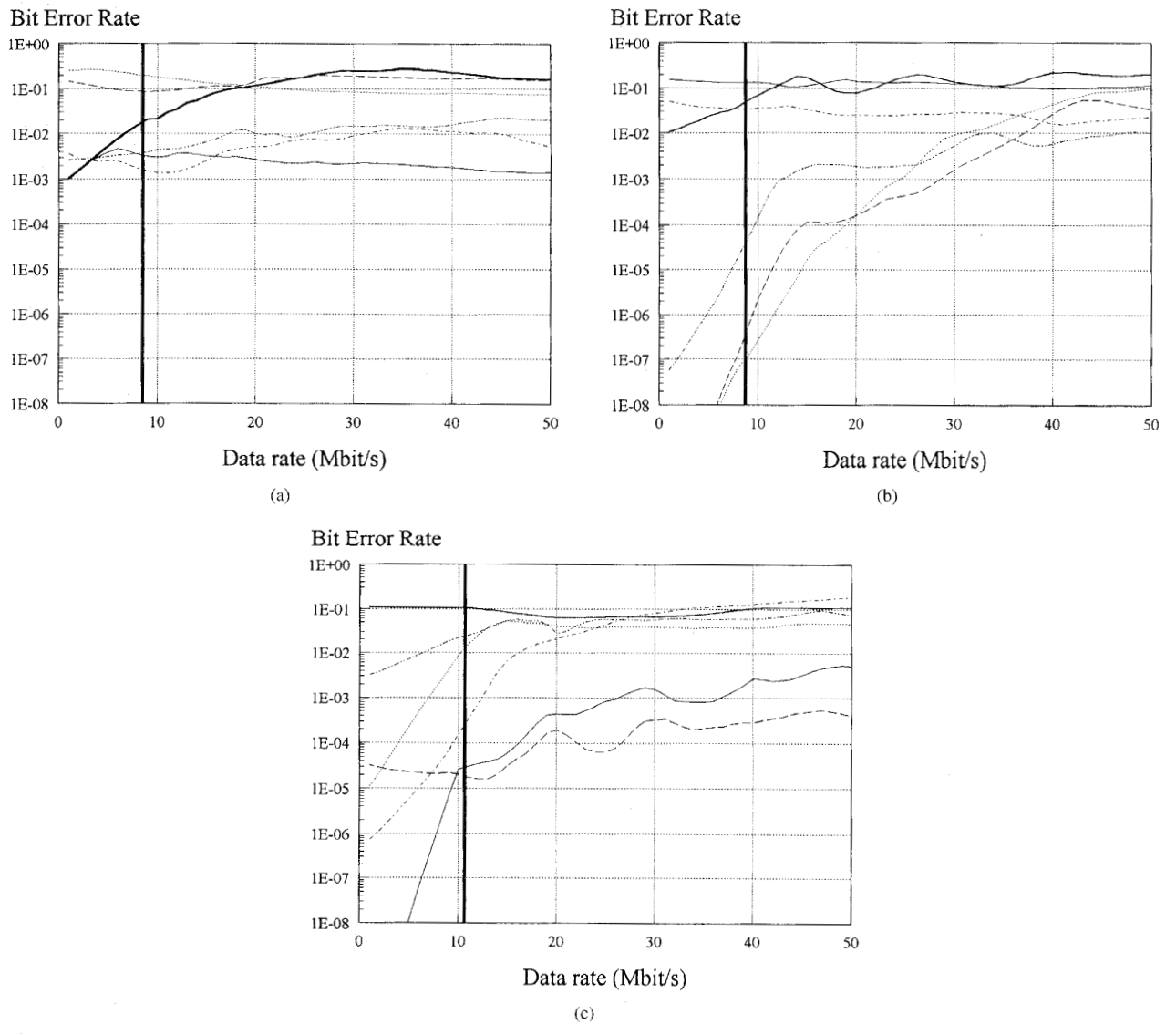

Fig. 19. BER as function of data rate in location CR (OBS), at: (a) 2.4 GHz; (b) 4.75 GHz; (c) 11.5 GHz. The different positions in the circular cluster are indicated as: 1: ____; 2: {−}{−}; 3: · · · · · ·; 4: -·-·-·-·-; 5: ____; 6: ·····. The bold vertical line indicates $R_{\max} = 1/4\overline{\tau}_{\rm rms}$.

bold lines in the figures indicate the bitrate $R_{\max} = 1/4\tau_{\rm rms}$. In general $\tau_{\rm rms}$ within a cluster does not show large variation. The calculated values of $R_{\max}$ for the different positions in a cluster are within 10% of the indicated average value of $R_{\max}$. The BER results show a large variation for constant bitrate at different positions in a cluster which do not differ more than a couple of wavelengths $(\lambda/2 - 4\lambda)$ in distance. Over such a small area the PDP, and therefore also $\tau_{\rm rms}$, does not change significantly (Fig. 6). These BER differences are therefore mainly caused by different combinations of path phases, which result in different frequency responses of the channel. In general, BER increases with increasing bitrate as expected, however, for a significant number of positions BER is nearly constant as function of bitrate, or even decreases with increasing bitrate. The reason for this unexpected behavior is that for those cases paths with different delays and phases add up more advantageous at the receiver for certain bitrates. From the BER results no clear difference is seen for different frequencies or even LOS and OBS situations. The large variation of channel performance, which is found when the antenna is moved over a distance in the order of the wavelength λ, can be exploited by antenna selection diversity, where the antenna with the best performance is chosen.

V. Conclusions

In this paper wideband channel measurement results for an indoor office environment at three frequencies: 2.4, 4.75, and 11.5 GHz are presented, and an analytical BER model for the stationary frequency selective multipath channel is derived.

1) Path-Loss: The parameters of a simple path-loss model have been determined. It can be concluded that this model gives accurate results for LOS situations. The values for the path-loss law exponent found for LOS paths are within the range 1.8–2.0 for all frequencies. In OBS situations the path-

loss law exponent increases with frequency and is 3.3, 3.8, and 4.5 at 2.4, 4.75, and 11.5 GHz, respectively. For OBS situations however, the attenuation predictions of the simple model are not very accurate.

2) Delay Spread $\tau_{\rm rms}$: The delay spread $\tau_{\rm rms}$has been determined for different types of rooms with different dimensions. $\tau_{\rm rms}$ increases for larger rooms. In the hall way very strong fluctuations were found. At 11.5 GHz $\tau_{\rm rms}$ in most cases is significantly smaller, about 30%, than at 2.4 GHz and 4.75 GHz, which are in general of about the same value. OBS paths show increased $\tau_{\rm rms}$ values when compared to LOS paths. In different situations, the median values of $\tau_{\rm rms}$ at 2.4 and 4.75 GHz range from 10–20 ns. At 11.5 GHz the median values $\tau_{\rm rms}$ ranges from 5–15 ns.

3) Coherence Bandwidth: The coherence bandwidth shows significant variation, also within a cluster of measurements. For the lower frequencies 40–45% of the clusters had at least one position with $B_{\rm coh} > 250$ MHz. At 11.5 GHz this percentage was even 65%. The relation $\alpha = 1/(\tau_{\rm rms} \cdot B_{\rm coh})$ shows large variation of α between 0.5 and 7. The median values of for LOS and OBS are about four and five, respectively.

4) Presence of People: The effects of people on path loss, when compared to the results for an empty room, is small. For LOS situations the effect is negligible. When people obstruct the direct path, 4–5.5 dB extra attenuation was found on the average. No clear difference in behavior was found for the three frequencies 2.4, 4.75, and 11.5 GHz. No influence of people on $\tau_{\rm rms}$ was found.

5) BER Results: A model has been developed to evaluate BER in a stationary frequency selective multipath channel for BPSK modulation. With this model, lower bound BER results have been calculated for a conventional coherent BPSK receiver, as a function of bitrate up to 50 Mb/s, at 2.4, 4.75, and 11.5 GHz. It was found that BER for constant bitrate varies significantly when the antenna is displaced over very small distances $(\lambda/2 - 4\lambda)$. This difference is mainly caused by relative phase changes of the paths. In general BER increases with bitrate, however this is not always the case. Many channels show a relatively constant BER or even a decreasing BER with increasing bitrate. The large variation in BER within a small cluster can be exploited by using antenna diversity.

Combined channel impulse response measurements and BER measurements are recommended to validate the BER model presented in this paper.

ACKNOWLEDGMENT

The authors are very grateful to the Physics and Electronics Laboratory of the Dutch Organization of Applied Scientific Research TNO, for performing the indoor coherent channel measurements, and making the measurement data available for further research at Delft University of Technology.

REFERENCES

[1] H. Zaghloul, G. Morrison, and M. Fattouche, "Frequency response and path-loss measurements of indoor channel," *Electron. Lett.*, vol. 27, no. 12, pp. 1021–1022, June 1991.

[2] S. Y. Seidel and T. S. Rappaport, "Path-loss prediction in multifloored buildings at 914 MHz," *Electron. Lett.*, pp. 1384–1387, vol. 27, no. 15, July 1991.

[3] D. M. J. Devasirvatham, C. Banerjee, R. R. Murray, and D. A. Rappaport, "Four-frequency radiowave propagation measurements of the indoor environment in a large metropolitan commercial building," in *Proc. IEEE GLOBECOM '91*, Phoenix, AZ, Dec. 1991, pp. 1282–1286.

[4] A. A. M. Saleh and R. A. Valenzuela, "A statistical model for indoor multipath propagation," *IEEE J. Select. Areas Commun.*, vol. CSA-5, no. 2, pp. 128–137, Feb. 1987.

[5] S. Y. Seidel and T. S. Rappaport, "Path-loss prediction in multifloored buildings at 914 MHz," *Electron. Lett.*, vol. 27, no. 15, pp. 1384–1387, July 1991.

[6] A. J. Motley and J. M. P. Keenan, "Personal communication radio coverage in buildings at 900 MHz and 1700 MHz," *Electron. Lett.*, vol. 24, no. 12, pp. 763–764, June 1988.

[7] S. J. Howard and K. Pahlavan, "Measurement and analysis of the indoor radio channel in the frequency domain," *IEEE Trans. Instrum. Meas.*, vol. 39, no. 5, pp. 751–755, Oct. 1990.

[8] ——, "Frequency domain measurements of indoor radio channels," *Electron. Lett.*, vol. 25, no. 24, pp. 1645–1647, Nov. 1989.

[9] G. J. M. Janssen and R. Prasad, "Propagation measurements in an indoor radio environment at 2.4 GHz, 4.75 GHz and 11.5 GHz," in *Proc. IEEE VTS Conf. '92*, Denver, CO, May 10–13, 1992, pp. 617–620.

[10] M. Kavehrad and B. Ramamurthi, "Direct-sequence spread spectrum with DPSK modulation and diversity for indoor wireless communication," *IEEE Trans. Commun.*, vol. COM-35, no. 2, pp. 224–236, Feb. 1987.

[11] A. Zigic and R. Prasad, "Bit error rate of decision feedback equaliser for indoor wireless communication," *Electron. Lett.*, vol. 28, pp 1949–1950, Oct. 1992.

[12] R. Prasad, A. Kegel, and M. B. Loog, "Cochannel interference probability for picocellular system with multiple Rician faded interferers," *Electron. Lett.*, vol. 28, pp. 2225–2226, Nov. 1992.

[13] H. S. Misser, A. Kegel, and R. Prasad, "Monte Carlo simulation of direct sequence spread spectrum for indoor radio communication in a Rician fading channel," *IEE Proc. I*, vol. 139, no. 6, pp. 620–624, Dec. 1992.

[14] J. C.-I. Chuang, "The effects of time delay spread on portable radio communications channels with digital modulation," *IEEE J. Select. Areas Commun.*, vol. SAC-5, no. 5, pp. 879–889, June 1987.

[15] D. C. Cox and R. P. Leck, "Correlation bandwidth and delay spread multipath propagation statistcs for 910 MHz urban mobile radio channels," *IEEE Trans. Commun.*, vol. COM-23, pp. 1271–1280, 1975.

[16] B. Glance and L. J. Greenstein, "Frequency selective fading effects in digital mobile radio with diversity combining," *IEEE Trans. Commun.*, vol. COM-31, no. 9, pp. 1085–1094, Sept. 1983.

[17] J. G. Proakis, *Digital Communications*, 2nd ed. New York: McGraw-Hill, 1989.

[18] W. C. Jakes, *Microwave Mobile Communications*. New York: Wiley, 1974.

[19] P. F. M. Smulders and A. G. Wagemans, "Mm-wave biconical horn antennas for near uniform coverage in indoor pico-cells," *Electron. Lett.*, vol. 28, pp. 679–681, Mar. 1992.

[20] F. M. Gardner, *Phaselock Techniques*, 2nd ed. New York: Wiley, 1979.

[21] G. J. M. Janssen, P. A. Stigter, and R. Prasad, "A model for bit error rate evaluation of indoor frequency selective channels using multipath measurement results at 2.4, 4.75 and 11.5 Ghz," in *Int. Zürich Seminar on Mobile Comm.*, Lect. Notes in Comp. Sc. 783, Mar. 1994, pp. 344–355.

[22] G. J. M. Janssen, B. C. v. Lieshout, and R. Prasad, "BER performance of millimeter wave indoor communication sytems using multiple antenna signals," in *IEEE Proc. Commun. Theory Mini-Conf. GLOBECOM'94*, San Francisco, Dec. 1994, pp. 105–109.

Gerard J. M. Janssen (M'93) received the M.Sc.E.E. degree from Eindhoven University of Technology, The Netherlands, in 1986.

After graduation, he joined the Physics and Electronics Laboratory of the Dutch Organization of Applied Scientific Research (TNO) where he was involved in research on radiometry, radar cross section modeling, radio direction finding, and wideband propagation measurements. In 1992, he joined Delft University of Technology as an Assistant Professor in the Telecommunications and Traffic Control Systems Group. Currently he is working toward the Ph.D. degree. His research interests are in narrowband and wideband robust multi-signal receivers, indoor radio propagation, and diversity techniques.

Patrick A. Stigter received the M.Sc. degree in electrical engineering from Delft University of Technology, The Netherlands, in 1993.

During his studies, he worked with the Physics and Electronics Laboratory of the Dutch Organization of Applied Scientific Research (TNO) where he was involved in indoor propagation measurements. His research interests are in indoor wireless communications.

Ramjee Prasad (M'88–SM'90) received the B.Sc. (Eng.) from Bihar Institute of Technology, Sindri, India, and the M.Sc. (Eng.), and Ph.D. degrees from Birla Institute of Technology (BIT), Ranchi, India, in 1968, 1970, and 1979, respectively.

He joined BIT as Senior Research Fellow in 1970 and became Associate Professor in 1980. During 1983–1988 he was with the University of Dar es Salaam (UDSM), Tanzania, where he became Full Professor in Telecommunications in the Department of Electrical Engineering in 1986. Since 1988, he has been with the Telecommunications and Traffic Control Systems Group, Delft University of Technology, The Netherlands, where he is actively involved in the area of personal, indoor and mobile radio communications. He has published over 200 technical papers and authored a book *CDMA For Wireless Personal Communications* Norwood, MA: Artech House. He is a Coordinating Editor and an Editor-in-Chief of *Wireless Personal Communications* and is also an editorial board member of *IEEE Communications Magazine* and *IEE Electronics Communication Engineering Journal*. His current research interest is in wireless networks, packet communications, adaptive equalizers, spread-spectrum CDMA systems, multimedia communications, and wireless ATM. He has presented tutorials on Mobile and Indoor Radio Communications at various universities, technical institutions, and IEEE conferences. He is also a member of a working group of European co-operation in the field of scientific and technical research project (COST-231) dealing with "Evolution of Land Mobile Radio (including personal) Communications" as an expert for the Netherlands. He is one of the lecturers of the Joint European Compact Course on "Mobile Personal Communication Systems."

Dr. Prasad is listed in the *Who's Who in the World*. He was Organizer and Interim Chairman of IEEE Vehicular Technology/Communications Society Joint Chapter, Benelux Section (now the elected chairman of the joint chapter). He is also founder of the IEEE Symposium on Communications and Vehicular Technology (SCVT) in the Benelux and he was the Symposium Chairman of SCVT'93. He was the Technical Program Chairman of PIMRC'94 International Symposium held in The Hague, The Netherlands and also of the Third Communication Theory Mini-Conference in conjunction with GLOBECOM'94 held in San Francisco, CA. He is a Fellow of IEE, a Fellow of the Institution of Electronics and Telecommunication Engineers, and a Member of The Netherlands Electronics and Radio Society (NERG).